

# BrainNetMLP: An Efficient and Effective Baseline for Functional Brain Network Classification

Jiacheng Hou<sup>1</sup>, Zhenjie Song<sup>1</sup>, and Ercan Engin Kuruoglu<sup>1</sup>

Tsinghua Shenzhen International Graduate School, Tsinghua University, China

**Abstract.** Recent studies have made great progress in functional brain network classification by modeling the brain as a network of Regions of Interest (ROIs) and leveraging their connections to understand brain functionality and diagnose mental disorders. Various deep learning architectures, including Convolutional Neural Networks, Graph Neural Networks, and the recent Transformer, have been developed. However, despite the increasing complexity of these models, the performance gain has not been as salient. This raises a question: *Does increasing model complexity necessarily lead to higher classification accuracy?* In this paper, we revisit the simplest deep learning architecture, the Multi-Layer Perceptron (MLP), and propose a pure MLP-based method, named BrainNetMLP, for functional brain network classification, which capitalizes on the advantages of MLP, including efficient computation and fewer parameters. Moreover, BrainNetMLP incorporates a dual-branch structure to jointly capture both spatial connectivity and spectral information, enabling precise spatiotemporal feature fusion. We evaluate our proposed BrainNetMLP on two public and popular brain network classification datasets, the Human Connectome Project (HCP) and the Autism Brain Imaging Data Exchange (ABIDE). Experimental results demonstrate pure MLP-based methods can achieve state-of-the-art performance, revealing the potential of MLP-based models as more efficient yet effective alternatives in functional brain network classification. The code will be available at <https://github.com/JayceonHo/BrainNetMLP>.

**Keywords:** Functional Brain Network Classification · fMRI · Brain Functional Connectivity · MLP · Transformer

## 1 Introduction

The human brain is an extremely complex system composed of numerous interacting regions. Investigating the organization and understanding the connectivity between different regions has long been a central goal of neuroscience, which is valuable in clinical analysis, diagnosis, and the corresponding treatment [3, 5, 28]. For this reason, tremendous effort has been put into functional brain network classification. Among various brain networks, the Functional Connectivity (FC) network based on functional Magnetic Resonance Imaging (fMRI) data is common and widely adopted [25]. Given a specific atlas, Regions of Interest (ROIs) can be separated from fMRI images and defined as nodes. The average Blood-Oxygen

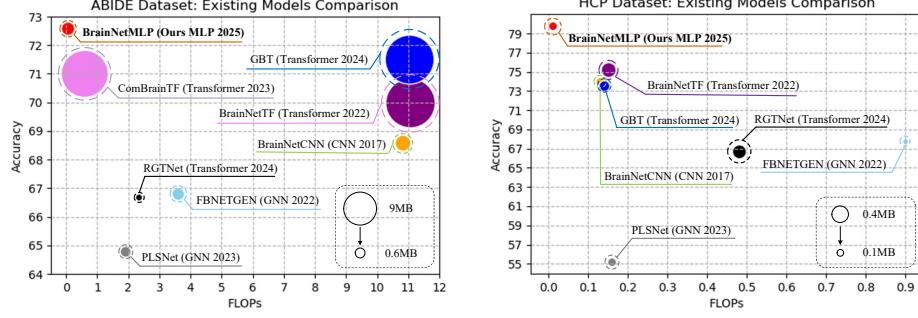


Fig. 1: Comparison of the existing state-of-the-art models and our proposed BrainNetMLP model on ABIDE dataset and HCP dataset. The size of the circles corresponds to the size of the models.

Level Dependent (BOLD) signal on each region is then extracted, and the statistical dependence between different regions is modeled as edges [19, 20]. In this way, a brain functional network is built, and the analysis of it can effectively assist the prediction of neurological disorder [1, 13] and cognitive state [17, 27].

With the success of deep learning, various deep learning models have been adapted and applied to brain functional network classification, such as Convolutional Neural Networks (CNN), Graph Neural Networks (GNN), and Transformer [14, 15, 30]. Among them, the Transformer has been favored mostly because of its strength in capturing long-range correlation of different ROIs [1, 13, 23]. However, as shown in Fig. 1, in comparison to the surge of model complexity, the performance gain of transformers is relatively marginal, which brings a question to us: *Does increasing model complexity necessarily lead to higher classification accuracy?*

Recently, the Multiple Layer Perceptron (MLP), a classical machine learning model, has been revisited, and a series of MLP-based models emerged as efficient yet effective alternatives to transformers in varying tasks [11, 21, 22, 26]. Compared to transformers, MLPs possess several inherent merits, such as lower computational cost and fewer parameters, which are desired properties in brain network classification, especially when dealing with large-scale networks. Furthermore, owing to its fully connected structure, like transformers, the MLP model is also able to learn the underlying relationship between distant ROIs.

Motivated by this, we explore the MLP structure and propose a pure MLP-based method, named BrainNetMLP. BrainNetMLP is a dual branch architecture that incorporates two types of MLPs, the Spatial Connectivity Mixer (SCMixer) and Spectrum ROI Mixer (SRMixer), to separately extract the discriminative features from FC and the filtered spectrum of the raw BOLD signals. Specifically, the SCMixer leverages the symmetric property of the Pearson functional network to save computation and employs an MLP to globally learn ROI connectivity. Then, different from previous methods [1, 6, 16], we additionally adopt spectral

information in our designed SRMixer to utilize the temporal dynamics via spectral filtering and learning. Finally, the learned spatial and spectral features are fused to collaboratively predict the analysis outcome. By exploiting the spatial connectivity of ROIs, their spectral dynamics, and the spatiotemporal correlation, higher accuracy is attained. Our contributions are summarized as follows:

- We propose the BrainNetMLP method for functional brain network classification, which is the first pure MLP-based method and owns the merits of MLP, including efficient computation (*i.e.*,  $10\times$  less FLOPs) and fewer parameters (*i.e.*,  $2\times$  fewer parameters) compared with state-of-the-art transformer models.
- BrainNetMLP not only leverages spatial connectivity information but also exploits effective spectral components of the brain network, thereby collaboratively capturing the spatiotemporal dynamics for precise analysis.
- We evaluate our proposed BrainNetMLP method on two popular and public functional brain network classification datasets: the HCP and ABIDE datasets, which show state-of-the-art performance compared with existing larger models. This reveals the potential of the MLP structure for functional brain network classification.

## 2 Method

### 2.1 Overview

**Problem definition.** In functional brain network classification, we begin by separating each fMRI brain scan into  $N$  ROIs. Subsequently, we construct the FC matrix  $\mathbf{X} \in \mathbb{R}^{N \times N}$  based on the average BOLD time series  $\mathbf{T} \in \mathbb{R}^{L \times N}$ , where  $L$  signifies the length of each time series. Each element within this matrix represents the Pearson correlation coefficient estimated between pairs of ROIs. The goal of the brain analysis model is to predict the label  $y$  (*e.g.*, the mental state) from the given connectome  $\mathbf{X}$  and time series  $\mathbf{T}$  of the subject.

**Model pipeline.** To solve this problem, we propose BrainNetMLP, the overall pipeline of which is depicted in Fig. 2. Specifically,  $\mathbf{X}$  and  $\mathbf{T}$  are respectively fed to SCMixer and SRMixer for spatial and spectrum feature extraction. Then, the extracted features are fused and sent to an MLP for prediction.

### 2.2 Spatial Connectivity Mixer

The connectome is a widely used feature for functional brain network classification, as the connectivity information it contains is a crucial attribute of the network. Previous transformer models [1, 12, 23] directly treat the connectome  $\mathbf{X}$  as a feature matrix. In these works, one dimension of  $\mathbf{X}$  is regarded as tokens, and the other dimension is regarded as channels. Although the transformer structure allows token and channel mixing by the self-attention and feed-forward layer separately, we argue that this separate processing scheme is neither efficient nor necessary. In essence, each element in  $\mathbf{X}$  represents the correlation between two

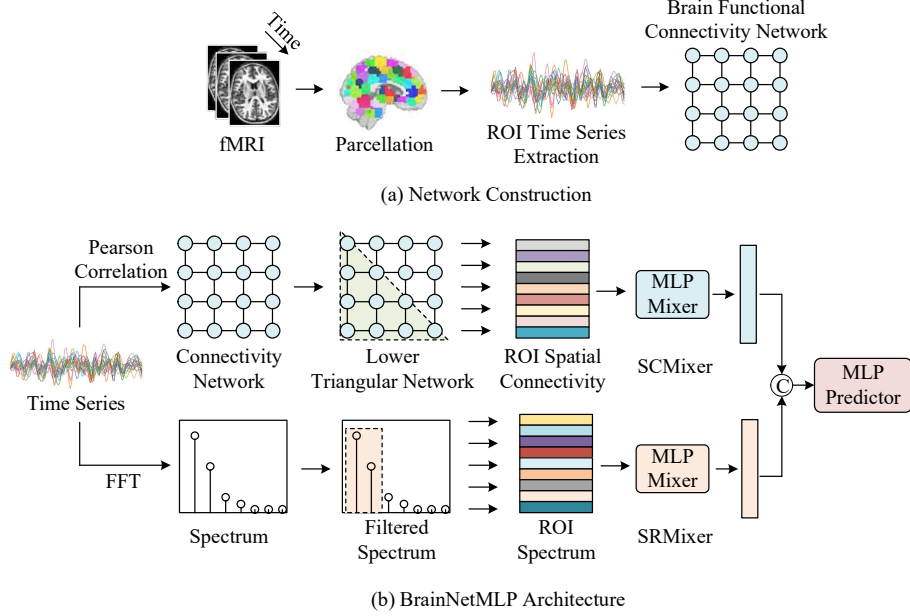


Fig. 2: The pipeline of our proposed BrainNetMLP framework, illustrating the (a) input data extraction and (b) the structure of our BrainNetMLP.

ROIs, the meaning of which is quite different from the features of transformers in computer vision (*e.g.*, images and videos) [9, 10] and natural language processing (*e.g.*, texts) [31, 32]. Thus, it is unnecessary to separately process elements of  $\mathbf{X}$  by different modules.

Based on this observation, the MLP structure becomes a good choice, as it can simultaneously and globally process all elements in the input. On the other hand, there is an important property of  $\mathbf{X}$  that has long been ignored by previous transformer-based brain network classification models [1, 13, 16], that is the symmetry of  $\mathbf{X}$ . The Pearson correlation is a commutable operation, which means  $\mathbf{X}[i, j] = \mathbf{X}[j, i]$ . Making use of this property can undoubtedly reduce the amount of computation. With these beliefs, in our designed SCMixer, we first extract the lower triangular (or upper triangular) matrix  $\mathbf{X}_{lower}$  from  $\mathbf{X}$ . Then it is flattened to a one-dimensional vector  $\mathbf{u} \in \mathbb{R}^{\frac{N(N+1)}{2}}$ :

$$\begin{aligned} \mathbf{X}_{lower} &= \text{TriExact}(\mathbf{X}), \\ \mathbf{u} &= \text{Flatten}(\mathbf{X}_{lower}), \end{aligned} \tag{1}$$

where “TriExtract” and “Flatten” represent the operations to extract the lower triangular matrix and flatten the matrix to a 1D vector.

In this way, the dimensionality of the to-be-processed feature (*i.e.*,  $\frac{N(N+1)}{2}$ ) is reduced to nearly half of the whole connectivity matrix (*i.e.*,  $N \times N$ ), which greatly saves computational resources. Besides, due to the symmetry property of

$\mathbf{X}$ , there is theoretically no loss of valid information. Then, a simple three-layered MLP (denoted by  $f_{con}$ ) is applied to  $\mathbf{u}$  for connectivity feature extraction:

$$\mathbf{x}_c = f_{con}(\mathbf{u}). \quad (2)$$

Generally,  $f_{con}$  plays the role of a learnable dimensionality reduction function, aiming to extract useful connectivity information and abandon non-discriminative connectivity information.

### 2.3 Spectrum ROIs Mixer

Besides the spatial connectivity information, an increasing number of works found that the network dynamics are also crucial [6, 29], as the human brain network is evolving with the change of mental states. A straightforward way to capture the dynamics is to leverage the time series  $\mathbf{T}$ . However, due to the variance and noise in different collection sites [13], we find that directly using  $\mathbf{T}$  for analysis would easily cause over-fitting. Hence, we choose to leverage the spectrum of  $\mathbf{T}$ , which is usually a more noise-robust feature representation. Specifically, in our developed SRMixer, we firstly apply the one-dimensional Fast Fourier Transform (FFT) on the temporal dimension of  $\mathbf{T}$  as:

$$\mathbf{S}_{real} = \text{FFT}(\mathbf{T}), \quad (3)$$

where  $\mathbf{S}_{real}$  represents half of the extracted spectrum (as the result of FFT for real number is symmetric). Then, we implement low-pass filtering on  $\mathbf{S}_{real}$  to filter out the noise, as the noise is usually high-frequency components, which can be expressed by:

$$\mathbf{S}_{real}^{low} = \mathcal{B}_{low}^k(\mathbf{S}_{real}), \quad (4)$$

where  $\mathcal{B}_{low}^k$  represents the low-pass filter, allowing only the first  $k$  frequency components to pass. Then, the amplitude of  $\mathbf{S}_{real}^{low}$  is sent to an MLP (denoted by  $f_{roi}$ ) for spectrum ROIs learning as:

$$\mathbf{X}_r = f_{roi}(|\mathbf{S}_{real}^{low}|), \quad (5)$$

where  $\mathbf{X}_r \in \mathbb{R}^{\frac{L \times H}{2}}$  denotes the learned spectrum features. Next, we average the spectrum features of different ROIs to obtain a more compact and comprehensive ROI feature representation as:

$$\mathbf{x}_r = \text{Mean}(\mathbf{X}_r), \quad (6)$$

where  $\mathbf{x}_r \in \mathbb{R}^H$  represents the averaged spectrum features of ROIs, and  $H$  signifies the hidden dimension.

### 2.4 Feature Fusion and Objective Function

After obtaining the features:  $\mathbf{x}_c$  and  $\mathbf{x}_r$  respectively extracted from ROIs spectrum and spatial connectivity. We employ a simple non-linear projection layer (denoted by  $\mathcal{P}$ ) as a predictor to jointly estimate the label  $\hat{y}$  as:

$$\hat{y} = \mathcal{P}(\text{GELU}(\text{Norm}([\mathbf{x}_c, \mathbf{x}_r]))), \quad (7)$$

where “GELU” and “Norm” represent the activation function [8] and normalization layers;  $[ \cdot , \cdot ]$  indicates the concatenation operation. Then, we employ the cross-entropy loss function as the objective function. As an efficient and effective baseline model, BrainNetMLP does not adopt additional loss functions to maintain its simplicity in implementation and comparison.

### 3 Experiments

#### 3.1 Experimental Settings

**Datasets.** We experiment on two widely used and different-sized functional brain network classification datasets: ABIDE and HCP datasets. The ABIDE dataset consists of 1035 resting-state functional MRI (rs-fMRI) collected from 17 different international sites [4]. Following previous works [1, 13], we use 1009 samples and parcel each fMRI into 200 ROIs based on the Craddock 200 atlas [2]. There are 516 subjects diagnosed with Autism Spectrum Disorder (ASD), and the remaining subjects are Healthy Control (HC) subjects. The HCP dataset consists of 1096 rs-fMRI collected from young adults aged from 22 to 35. We follow the preprocessing and division of the previous work and parcel the brain into 22 ROIs [6].

**Implementation Details.** Following previous works [1, 13, 16], for the ABIDE dataset, we split 70% of the subjects into the training set, 10% of the subjects into the validation set, and the remaining as the test set. For the HCP dataset, we follow the division provided by [6]. We train our model on both datasets with 200 epochs at a learning rate of  $1 \times 10^{-4}$ . All the experiments are run on a single NVIDIA RTX 4090 with 24GB of memory.

**Baseline.** We compare the performance of our proposed BrainNetMLP with state-of-the-art methods in a wide range of structures: 1) *CNN-based method*: A four-layered bottleneck CNN and BrainNetCNN [14]; 2) *GNN-based models*: STGCN [6], BrainGNN [15], FBNETGEN [12] and PLSNet [24]; 3) *Transformer-based models*: BrainNetTF [13], ComBrainTF [1], RGTNet [23] and GBT [16].

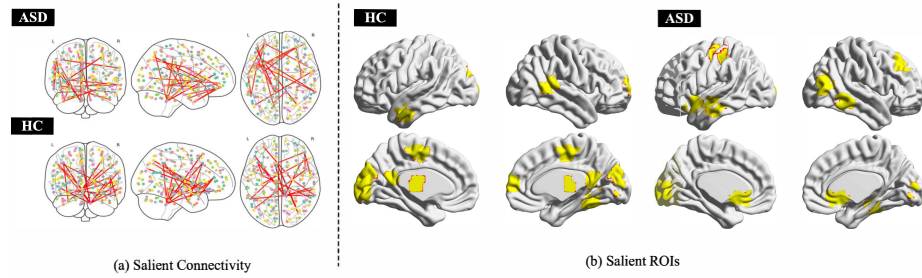


Fig. 3: Left and right respectively show the salient connectivity and ROIs detected by our method.

Table 1: Quantitative performance comparison with baselines on HCP and ABIDE datasets (Mean $\pm$ standard deviation). The best is shown in bold black.

Method	Structure	Dataset: ABIDE				Dataset: HCP			
		Accuracy	AUCROC	Specificity	Sensitivity	Accuracy	AUCROC	Specificity	Sensitivity
VanillaCNN	CNN	65.6 $\pm$ 1.7	72.6 $\pm$ 2.0	66.1 $\pm$ 1.7	68.9 $\pm$ 4.2	71.4 $\pm$ 2.1	79.3 $\pm$ 2.8	74.2 $\pm$ 3.1	68.9 $\pm$ 3.8
BrainNetCNN [14]	CNN	68.6 $\pm$ 1.2	69.9 $\pm$ 5.0	68.5 $\pm$ 6.9	71.7 $\pm$ 5.9	74.0 $\pm$ 1.8	82.6 $\pm$ 2.2	72.5 $\pm$ 10.4	<b>77.0<math>\pm</math>11.6</b>
STGCN* [6]	GNN	-	-	-	-	77.7 $\pm$ 3.2	86.9 $\pm$ 2.5	82.5 $\pm$ 4.3	72.2 $\pm$ 3.3
BrainGNN [15]	GNN	60.1 $\pm$ 2.6	65.6 $\pm$ 0.9	43.5 $\pm$ 9.4	<b>77.1<math>\pm</math>6.2</b>	62.5 $\pm$ 3.1	65.4 $\pm$ 4.0	73.0 $\pm$ 13.0	49.3 $\pm$ 14.4
FBNETGEN [12]	GNN	66.8 $\pm$ 1.9	74.8 $\pm$ 1.0	72.5 $\pm$ 5.1	62.2 $\pm$ 7.0	67.8 $\pm$ 4.7	74.6 $\pm$ 3.7	70.8 $\pm$ 5.3	64.9 $\pm$ 3.9
PLSNet [24]	GNN	64.8 $\pm$ 1.1	71.8 $\pm$ 2.3	67.1 $\pm$ 2.5	64.2 $\pm$ 2.7	55.2 $\pm$ 4.6	58.5 $\pm$ 4.3	63.2 $\pm$ 6.7	46.8 $\pm$ 9.3
BrainNetTF [13]	Transformer	70.0 $\pm$ 2.3	79.1 $\pm$ 1.1	68.3 $\pm$ 4.7	72.7 $\pm$ 1.0	75.2 $\pm$ 2.1	82.5 $\pm$ 1.6	81.0 $\pm$ 6.1	69.6 $\pm$ 6.4
ComBrainTF* [1]	Transformer	71.0 $\pm$ 1.5	77.2 $\pm$ 0.6	70.9 $\pm$ 4.3	72.6 $\pm$ 3.8	-	-	-	-
RGTNet [23]	Transformer	66.7 $\pm$ 2.8	73.4 $\pm$ 1.2	67.5 $\pm$ 1.8	65.6 $\pm$ 5.6	63.6 $\pm$ 1.2	68.4 $\pm$ 1.7	69.7 $\pm$ 4.4	56.2 $\pm$ 3.3
GBT [16]	Transformer	71.5 $\pm$ 2.1	<b>79.2<math>\pm</math>0.4</b>	69.5 $\pm$ 4.3	72.9 $\pm$ 3.5	73.6 $\pm$ 2.3	81.4 $\pm$ 2.6	80.1 $\pm$ 7.2	66.7 $\pm$ 9.0
BrainNetMLP	MLP	<b>72.6<math>\pm</math>1.7</b>	78.4 $\pm$ 0.1	<b>72.5<math>\pm</math>2.7</b>	73.7 $\pm$ 1.4	<b>79.8<math>\pm</math>1.7</b>	<b>88.1<math>\pm</math>1.5</b>	<b>83.1<math>\pm</math>3.4</b>	76.8 $\pm$ 4.1

\* STGCN and ComBrainTF require fixed adjacency matrices and community priors, which are not provided in the ABIDE and HCP datasets.

Table 2: Ablation study on the architecture of our proposed BrainNetMLP.

Method	Dataset: ABIDE				Dataset: HCP			
	Accuracy	AUCROC	Specificity	Sensitivity	Accuracy	AUCROC	Specificity	Sensitivity
w/o. SCMixer	52.2 $\pm$ 1.5	51.9 $\pm$ 2.3	34.0 $\pm$ 8.0	<b>74.0<math>\pm</math>7.5</b>	61.6 $\pm$ 2.9	66.0 $\pm$ 3.0	62.2 $\pm$ 2.8	62.1 $\pm$ 6.5
w/o. SRMixer	62.0 $\pm$ 6.1	75.0 $\pm$ 1.8	<b>77.0<math>\pm</math>17.5</b>	48.5 $\pm$ 27.6	77.6 $\pm$ 2.9	86.4 $\pm$ 1.4	82.0 $\pm$ 1.3	73.6 $\pm$ 6.5
w/o. filtering*	71.8 $\pm$ 1.5	78.4 $\pm$ 0.3	71.7 $\pm$ 1.6	73.5 $\pm$ 2.2	78.6 $\pm$ 1.9	87.6 $\pm$ 1.6	81.1 $\pm$ 2.4	76.8 $\pm$ 5.0
Full model	<b>72.6<math>\pm</math>1.7</b>	<b>78.4<math>\pm</math>0.1</b>	72.5 $\pm$ 2.7	73.7 $\pm$ 1.4	<b>79.8<math>\pm</math>1.7</b>	<b>88.1<math>\pm</math>1.5</b>	<b>83.1<math>\pm</math>3.4</b>	<b>76.8<math>\pm</math>4.1</b>

\* filtering means only removing the low-pass filter  $B_{low}^k$  in SRMixer.

### 3.2 Results Analysis

**Quantitative comparison.** 1) *Performance comparison:* We compare the performance quantitatively in Table 1, where it can be seen that BrainNetMLP achieves state-of-the-art performance on both datasets. Specifically, on the ABIDE dataset, BrainNetMLP improves the accuracy by around 1.1% and realizes comparative AUCROC compared with the second-best model. On the HCP dataset, BrainNetMLP yields a 2.1% improvement in accuracy and a 1.2% increase in AUCROC, observably outperforming the second-best model. This can be attributed to the additionally incorporated spectral information in BrainNetMLP, which has been ignored by the existing methods (*e.g.*, GBT and BrainNetTF).

2) *Complexity comparison:* As compared in Fig. 1, the consumed computational cost (FLOPs) and the number of learnable parameters are all significantly fewer than the state-of-the-art transformers. Moreover, with the expansion of the network (*i.e.*, from 22 ROIs per network in the HCP dataset to 200 ROIs per network in the ABIDE dataset), unlike the rapid increase of complexity in the GBT (0.14G/0.21M  $\rightarrow$  11.04G/8.89M) and BrainNetTF (0.15G/0.4M  $\rightarrow$  11.06G/9.08M), our BrainNetMLP exhibits more advanced scalability (0.01G/0.14M  $\rightarrow$  0.06G/0.65M).

**Interpretability of BrainNetMLP.** Besides quantitative results, we also visualize how does BrainNetMLP make decisions on the ABIDE dataset. Particularly,



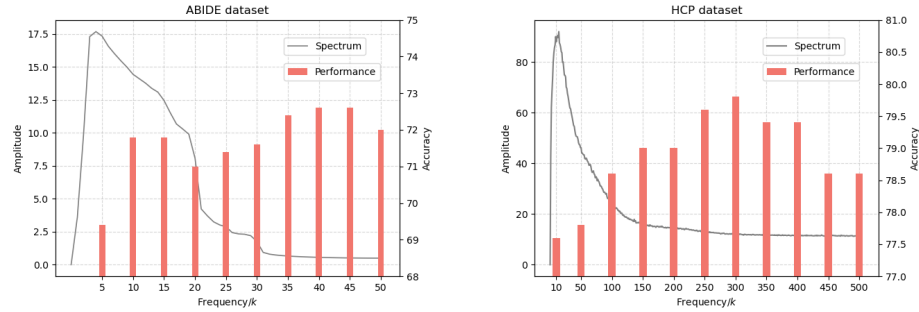


Fig. 4: The line chart (left axis) and the bar chart (right axis) present the visualized spectrum and the model accuracy to varying  $k$ .

we generate the saliency maps [18] in Fig. 3 respectively based on the gradients of the SCMixer and SRMixer modules, which visualizes the salient connectivity/ROIs for ASD and HC subjects. From Fig. 3, we can find the major difference exhibited in the DMN and SMN, which is in accordance with other research on ASD [7].

### 3.3 Ablation Study

**Ablation study on network architecture.** As reported in Table 2, on both datasets, no matter which component is removed, the overall performance is worse than the full model. Notably, on the ABIDE dataset, solely employing SCMixer or SRMixer can achieve the best specificity and sensitivity, which shows SCMixer and SRMixer can respectively assist in decreasing the rate of false-alarm and miss-detect. As a result, it can be observed that adaptively combining them complementarily improves the overall performance of the full model.

**Ablation study on spectrum filter.** In SRMixer, we adopt a low-pass filter to remove invalid frequency components. From Table 2, without filtering, the accuracy on both datasets is reduced by around 0.8% and 1.2% separately. The hyper-parameter  $k$  of the filter determines which frequency components are used for learning. The visualized spectrum and performance of different selections of  $k$  are shown in Fig. 4, where we can find selecting a suitable  $k$  can keep valid frequency information and filter out noise, effectively boosting the performance.

## 4 Conclusion

In this paper, we propose the first MLP-only method, named BrainNetMLP, for functional brain network classification. Owing to the simplicity of the MLP structure, it is superior in efficiency and scalability, with more than one order of magnitude reduction in computational complexity compared with the state-of-the-art transformer models. Besides, different from the previous method, we



design a dual branch architecture, which not only utilizes spatial connectivity but also exploits spectral features with adaptive feature fusion. In this way, BrainNetMLP can fully leverage spatial and temporal discriminative features for analysis, producing advanced performance on the ABIDE and HCP datasets. The experimental results illustrate the significant untapped potential of the MLP structure in functional brain network classification and outline an efficient yet effective alternative to the current brain transformers.

## References

1. Bannadabhavi, A., Lee, S., Deng, W., Ying, R., Li, X.: Community-aware transformer for autism prediction in fmri connectome. In: Medical Image Computing and Computer-Assisted Intervention. pp. 287–297. Springer (2023)
2. Craddock, R.C., James, G.A., Holtzheimer III, P.E., Hu, X.P., Mayberg, H.S.: A whole brain fmri atlas generated via spatially constrained spectral clustering. *Human Brain Mapping* **33**(8), 1914–1928 (2012)
3. Deco, G., Jirsa, V.K., McIntosh, A.R.: Emerging concepts for the dynamical organization of resting-state activity in the brain. *Nature Reviews Neuroscience* **12**(1), 43–56 (2011)
4. Di Martino, A., Yan, C.G., Li, Q., Denio, E., Castellanos, F.X., Alaerts, K., Anderson, J.S., Assaf, M., Bookheimer, S.Y., Dapretto, M., et al.: The autism brain imaging data exchange: Towards a large-scale evaluation of the intrinsic brain architecture in autism. *Molecular Psychiatry* **19**(6), 659–667 (2014)
5. Fornito, A., Zalesky, A., Bullmore, E.: *Fundamentals of Brain Network Analysis*. Academic Press (2016)
6. Gadgil, S., Zhao, Q., Pfefferbaum, A., Sullivan, E.V., Adeli, E., Pohl, K.M.: Spatio-temporal graph convolution for resting-state fmri analysis. In: Medical Image Computing and Computer Assisted Intervention. pp. 528–538. Springer (2020)
7. Harikumar, A., Evans, D.W., Dougherty, C.C., Carpenter, K.L., Michael, A.M.: A review of the default mode network in autism spectrum disorders and attention deficit hyperactivity disorder. *Brain connectivity* **11**(4), 253–263 (2021)
8. Hendrycks, D., Gimpel, K.: Gaussian error linear units (gelus). arXiv preprint arXiv:1606.08415 (2016)
9. Hou, J., Ji, Z., Yang, J., Wang, C., Zheng, F.: Mcd-net: toward rgb-d video inpainting in real-world scenes. *IEEE Transactions on Image Processing* **33**, 1095–1108 (2024)
10. Hou, J., Ji, Z., Yang, J., Zheng, F.: Bidirectional error-aware fusion network for video inpainting. *IEEE Transactions on Circuits and Systems for Video Technology* (2024)
11. Hu, Y., You, H., Wang, Z., Wang, Z., Zhou, E., Gao, Y.: Graph-mlp: Node classification without message passing in graph. arXiv preprint arXiv:2106.04051 (2021)

12. Kan, X., Cui, H., Lukemire, J., Guo, Y., Yang, C.: Fbnetgen: Task-aware gnn-based fmri analysis via functional brain network generation. In: International Conference on Medical Imaging with Deep Learning. pp. 618–637. PMLR (2022)
13. Kan, X., Dai, W., Cui, H., Zhang, Z., Guo, Y., Yang, C.: Brain network transformer. *Advances in Neural Information Processing Systems* **35**, 25586–25599 (2022)
14. Kawahara, J., Brown, C.J., Miller, S.P., Booth, B.G., Chau, V., Grunau, R.E., Zwicker, J.G., Hamarneh, G.: Brainnetcnn: Convolutional neural networks for brain networks; towards predicting neurodevelopment. *NeuroImage* **146**, 1038–1049 (2017)
15. Li, X., Zhou, Y., Dvornek, N., Zhang, M., Gao, S., Zhuang, J., Scheinost, D., Staib, L., Ventola, P., Duncan, J.: Brainngn: Interpretable brain graph neural network for fmri analysis. *bioRxiv* (2020)
16. Peng, Z., He, Z., Jiang, Y., Wang, P., Yuan, Y.: Gbt: Geometric-oriented brain transformer for autism diagnosis. In: Medical Image Computing and Computer-Assisted Intervention. pp. 142–152 (2024)
17. Satterthwaite, T.D., Wolf, D.H., Roalf, D.R., Ruparel, K., Erus, G., Vandekar, S., Gennatas, E.D., Elliott, M.A., Smith, A., Hakonarson, H., et al.: Linked sex differences in cognition and functional connectivity in youth. *Cerebral Cortex* **25**(9), 2383–2394 (2015)
18. Simonyan, K., Vedaldi, A., Zisserman, A.: Deep inside convolutional networks: Visualising image classification models and saliency maps. *arXiv preprint arXiv:1312.6034* (2013)
19. Simpson, S.L., Bowman, F.D., Laurienti, P.J.: Analyzing complex functional brain networks: Fusing statistics and network science to understand the brain. *Statistics Surveys* **7**, 1 (2013)
20. Smith, S.M., Miller, K.L., Salimi-Khorshidi, G., Webster, M., Beckmann, C.F., Nichols, T.E., Ramsey, J.D., Woolrich, M.W.: Network modelling methods for fmri. *NeuroImage* **54**(2), 875–891 (2011)
21. Tolstikhin, I.O., Houlsby, N., Kolesnikov, A., Beyer, L., Zhai, X., Unterthiner, T., Yung, J., Steiner, A., Keysers, D., Uszkoreit, J., et al.: Mlp-mixer: An all-mlp architecture for vision. *Advances in Neural Information Processing Systems* **34**, 24261–24272 (2021)
22. Wang, S., Li, J., Shi, X., Ye, Z., Mo, B., Lin, W., Ju, S., Chu, Z., Jin, M.: Timemixer++: A general time series pattern machine for universal predictive analysis. In: International Conference on Learning Representation (2024)
23. Wang, Y., Long, H., Bo, T., Zheng, J.: Residual graph transformer for autism spectrum disorder prediction. *Computer Methods and Programs in Biomedicine* **247**, 108065 (2024)
24. Wang, Y., Long, H., Zhou, Q., Bo, T., Zheng, J.: Plsnet: Position-aware gcn-based autism spectrum disorder diagnosis via fc learning and rois sifting. *Computers in Biology and Medicine* **163**, 107184 (2023)
25. Wang, Y., Kang, J., Kemmer, P.B., Guo, Y.: An efficient and reliable statistical method for estimating functional connectivity in large scale brain networks using partial correlation. *Frontiers in Neuroscience* **10**, 123 (2016)

26. Wang, Z., Jiang, W., Zhu, Y.M., Yuan, L., Song, Y., Liu, W.: Dynamixer: A vision mlp architecture with dynamic mixing. In: International Conference on Machine Learning. pp. 22691–22701. PMLR (2022)
27. Weis, S., Patil, K.R., Hoffstaedter, F., Nostro, A., Yeo, B.T., Eickhoff, S.B.: Sex classification by resting state brain connectivity. *Cerebral Cortex* **30**(2), 824–835 (2020)
28. Wig, G.S., Schlaggar, B.L., Petersen, S.E.: Concepts and principles in the analysis of brain networks. *Annals of the New York Academy of Sciences* **1224**(1), 126–146 (2011)
29. Yan, J., Chen, Y., Yang, S., Zhang, S., Jiang, M., Zhao, Z., Zhang, T., Zhao, Y., Becker, B., Liu, T., et al.: Multi-head gagnn: A multi-head guided attention graph neural network for modeling spatio-temporal patterns of holistic brain functional networks. In: Medical Image Computing and Computer Assisted Intervention. pp. 564–573. Springer (2021)
30. Yan, Y., Hou, J., Song, Z., Kuruoglu, E.E.: Signal processing over time-varying graphs: A systematic review. *arXiv preprint arXiv:2412.00462* (2024)
31. Yu, J., Li, J., Yu, Z., Huang, Q.: Multimodal transformer with multi-view visual representation for image captioning. *IEEE transactions on circuits and systems for video technology* **30**(12), 4467–4480 (2019)
32. Zhang, J., Chang, W.C., Yu, H.F., Dhillon, I.: Fast multi-resolution transformer fine-tuning for extreme multi-label text classification. *Advances in Neural Information Processing Systems* **34**, 7267–7280 (2021)